Apical targeting of syntaxin 3 is essential for epithelial cell polarity

Nikunj Sharma,[1,3] Seng Hui Low,[1,2] Saurav Misra,[4] Bhattaram Pallavi,[1] and Thomas Weimbs[1,2]

[1]Department of Molecular, Cellular, and Developmental Biology, [2]Neuroscience Research Institute, University of California, Santa Barbara, Santa Barbara, CA 93106
[3]Department of Biological, Geological, and Environmental Sciences, Cleveland State University, Cleveland, OH 44115
[4]Department of Molecular Cardiology, Lerner Research Institute, The Cleveland Clinic, Cleveland, OH 44195

In polarized epithelial cells, syntaxin 3 localizes to the apical plasma membrane and is involved in membrane fusion of apical trafficking pathways. We show that syntaxin 3 contains a necessary and sufficient apical targeting signal centered around a conserved FMDE motif. Mutation of any of three critical residues within this motif leads to loss of specific apical targeting. Modeling based on the known structure of syntaxin 1 revealed that these residues are exposed on the surface of a three-helix bundle. Syntaxin 3 targeting does not require binding to Munc18b. Instead, syntaxin 3 recruits Munc18b to the plasma membrane. Expression of mislocalized mutant syntaxin 3 in Madin-Darby canine kidney cells leads to basolateral mistargeting of apical membrane proteins, disturbance of tight junction formation, and loss of ability to form an organized polarized epithelium. These results indicate that SNARE proteins contribute to the overall specificity of membrane trafficking in vivo, and that the polarity of syntaxin 3 is essential for epithelial cell polarization.

Introduction

The majority of cell types in multicellular organisms are polarized and face two different environments. For example, epithelial cells face the outside world or lumen of an organ on one side, and the interstitial environment and basement membrane on the other. These cells exhibit functional and structural asymmetry in their apical and basolateral plasma membranes that is essential to their function. Epithelial cell polarity depends on the accurate targeting of apical and basolateral plasma membrane proteins (Mostov et al., 2003; Rodriguez-Boulan et al., 2005). Targeting information is usually present in the cargo proteins themselves. These targeting signals are thought to be recognized in the TGN or endosomes, which leads to the sorting of cargo proteins into transport vesicles destined for the apical or basolateral plasma membrane.

Like most intracellular membrane fusion events, vesicle fusion with the apical and basolateral plasma membranes is mediated by the SNARE machinery (Weimbs et al., 1997a; Mostov et al., 2003). Mammals express >30 different members of the SNARE superfamily, each one of them associated with a particular fusion event (Chen and Scheller, 2001; Jahn et al., 2003; Ungar and Hughson, 2003). SNAREs are characterized by one or two conserved SNARE motifs of ~60 amino acids (Weimbs et al., 1997b, 1998) that mediate the SNARE–SNARE interactions. SNARE complexes contain at least one member of the syntaxin family, in addition to two or three other cognate SNAREs. SNARE pairing was initially proposed to contribute to the overall specificity of membrane trafficking pathways (Rothman and Warren, 1994). Using in vitro–reconstituted fusion assays, it has been demonstrated that only matching combinations of cognate SNAREs lead to successful membrane fusion (McNew et al., 2000; Scales et al., 2000). An important question is whether SNAREs, indeed, contribute to specificity of trafficking in living cells.

Epithelial cells generally contain at least two different plasma membrane syntaxins. Syntaxins 3 and 4 localize to the apical and basolateral plasma membranes, respectively, in virtually all epithelial cell types investigated to date. This includes the MDCK cell line (Low et al., 1996), all epithelial cell types along the renal tubule in vivo (Li et al., 2002), and a range of epithelial cells from other tissues (Weimbs et al., 1997a). Syntaxin 3 is involved in biosynthetic trafficking from the TGN to the apical plasma membrane and in apical recycling (Low et al., 1998a). Syntaxin 4 functions in trafficking from the TGN to the basolateral plasma membrane (Lafont et al., 1999). The high degree of conservation of the polarity of syntaxin 3 and 4 suggests that their function and proper localization may play an important role in epithelial polarization.

Correspondence to Thomas Weimbs: weimbs@lifesci.ucsb.edu

Abbreviations used in this paper: DOX, doxycycline; TEER, transepithelial electrical resistance.

The Journal of Cell Biology, Vol. 173, No. 6, June 19, 2006 937–948
http://www.jcb.org/cgi/doi/10.1083/jcb.200603132

The clear distinction between apical and basolateral trafficking pathways makes epithelial cells a good system in which to test the central prediction of the SNARE hypothesis on their contribution to the overall specificity of trafficking pathways. For example, one would predict that mislocalization of the apical syntaxin 3 to the basolateral domain would allow the inappropriate fusion of apical transport vesicles with that domain and reduce the fidelity of polarized trafficking. This is supported by our previous results; disruption of microtubules leads to partial mislocalization of syntaxin 3 to the basal membrane. Under these conditions, post-Golgi transport vesicles carrying apical cargo are able to fuse with the basal membrane (Kreitzer et al., 2003). Although these results were consistent with the idea that syntaxin 3 must be restricted to the apical membrane to achieve maximal fidelity of apical cargo transport, it could not be excluded that the observed cargo mistargeting was an indirect effect of microtubule disruption. To more fully test the contribution of apically localized syntaxin 3 to the fidelity of polarized trafficking, we have now investigated the mechanism of apical targeting of syntaxin 3. We report that syntaxin 3 contains a necessary and sufficient apical targeting signal in its NH_2-terminal helical domain and that disruption of this signal leads to the random localization of syntaxin 3 at the apical and basolateral domain. Expression of mislocalized syntaxin 3 results in mistargeting of apical cargo proteins and in the overall disruption of epithelial cell polarity. These results indicate that proper SNARE pairing, indeed, contributes to the specificity of membrane trafficking pathways in vivo. Furthermore, these results show that epithelial cell polarity is dependent not only on the function of syntaxin 3 but also on its polarity.

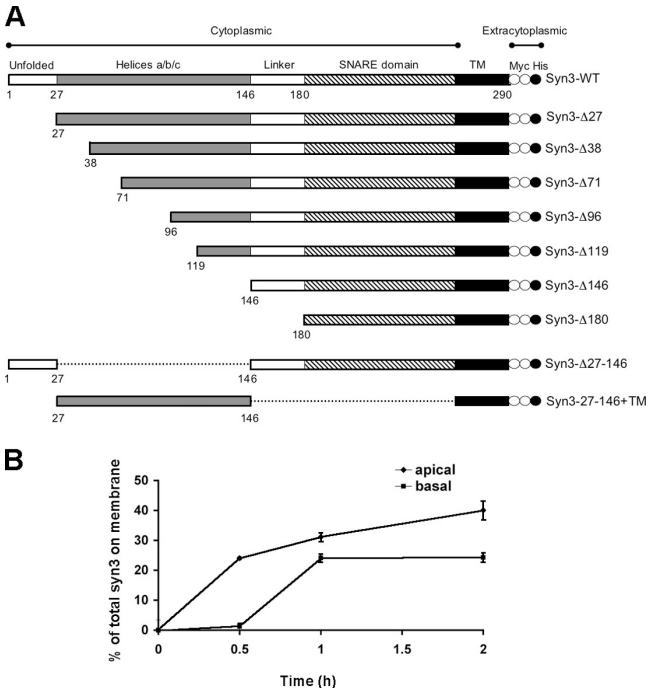

Figure 1. **Kinetics of surface targeting of syntaxin 3.** (A) Schematic of syntaxin 3 constructs. Domains are based on the structure of syntaxin 1A. Two myc epitope tags (white circles) and one His_6 tag (black circles) were added to the COOH termini. (B) Polarized MDCK cells stably expressing myc-tagged syntaxin 3 were metabolically labeled for 15 min with [^{35}S]methionine, followed by a chase for the indicated periods of time. Anti-myc antibody was present throughout the chase in the apical or basolateral media compartment. The percentage of surface-delivered, antibody-captured syntaxin 3 was quantified by immunoprecipitation, SDS-PAGE, and radio-analysis (see Materials and methods). Results are expressed as the percent of total radiolabeled syntaxin 3 that had reached the apical or basolateral surface at the given time (averages of triplicates ± SD; representative of three independent experiments).

Results

Apical targeting of syntaxin 3 in MDCK cells

At steady state, syntaxin 3 is highly enriched at the apical plasma membrane domain of MDCK cells (Low et al., 1996). To test whether newly synthesized syntaxin 3 is sorted in the biosynthetic pathway and directly delivered to the apical membrane, we established an assay based on pulse-chase metabolic labeling and detection of syntaxin 3 at the surface. Syntaxin 3 lacks an extracytoplasmic domain. To enable the detection of surface-delivered syntaxin 3 in intact cells, we engineered a fusion protein containing two COOH-terminal myc epitope tags (Fig. 1 A). We have previously shown that the added epitope tags are accessible to binding by anti-myc antibody in intact cells and do not interfere with the apical targeting of wild-type syntaxin 3 (Kreitzer et al., 2003). MDCK cells that were stably transfected with this syntaxin 3 fusion protein were cultured on permeable filter supports to establish polarized monolayers. Cells were pulse-labeled with [^{35}S]methionine, and newly synthesized syntaxin 3 was chased to the surface for different periods of time in the presence of anti-myc antibody in either the apical or basolateral media compartment to capture surface-delivered syntaxin 3. Successive immunoprecipitation of antibody-tagged and untagged radiolabeled syntaxin 3 allows quantitation of the kinetics of surface delivery (see Materials and methods). As shown in Fig. 1 B, although syntaxin 3 delivery is primarily apical, a significant fraction is also initially targeted to the basolateral domain. This suggests that syntaxin 3 undergoes sorting both during the initial delivery and at a later step, presumably after endocytosis from the basolateral membrane.

Identification of the apical targeting signal of syntaxin 3

Most apical targeting signals have been identified within extracytoplasmic domains of membrane proteins. Because syntaxin 3 does not contain an extracytoplasmic domain, its apical targeting must be specified by a determinant within the cytoplasmic or transmembrane domains. To identify an apical targeting signal of syntaxin 3, we generated mutants with successively deleted domains. Structural domains of syntaxin 3 were identified by sequence alignment with the highly homologous syntaxin 1 whose structure has been previously reported (Fernandez et al., 1998; Sutton et al., 1998; Lerman et al., 2000; Misura et al., 2000). Five domains are identified (Fig. 1 A) as follows: an unfolded NH_2-terminal domain is followed by a bundle of three α helices (H_{abc}), an unfolded linker domain, the SNARE domain, and the COOH-terminal transmembrane domain. Deletion of the NH_2-terminal unfolded domain (Syn3-Δ27) has no effect on

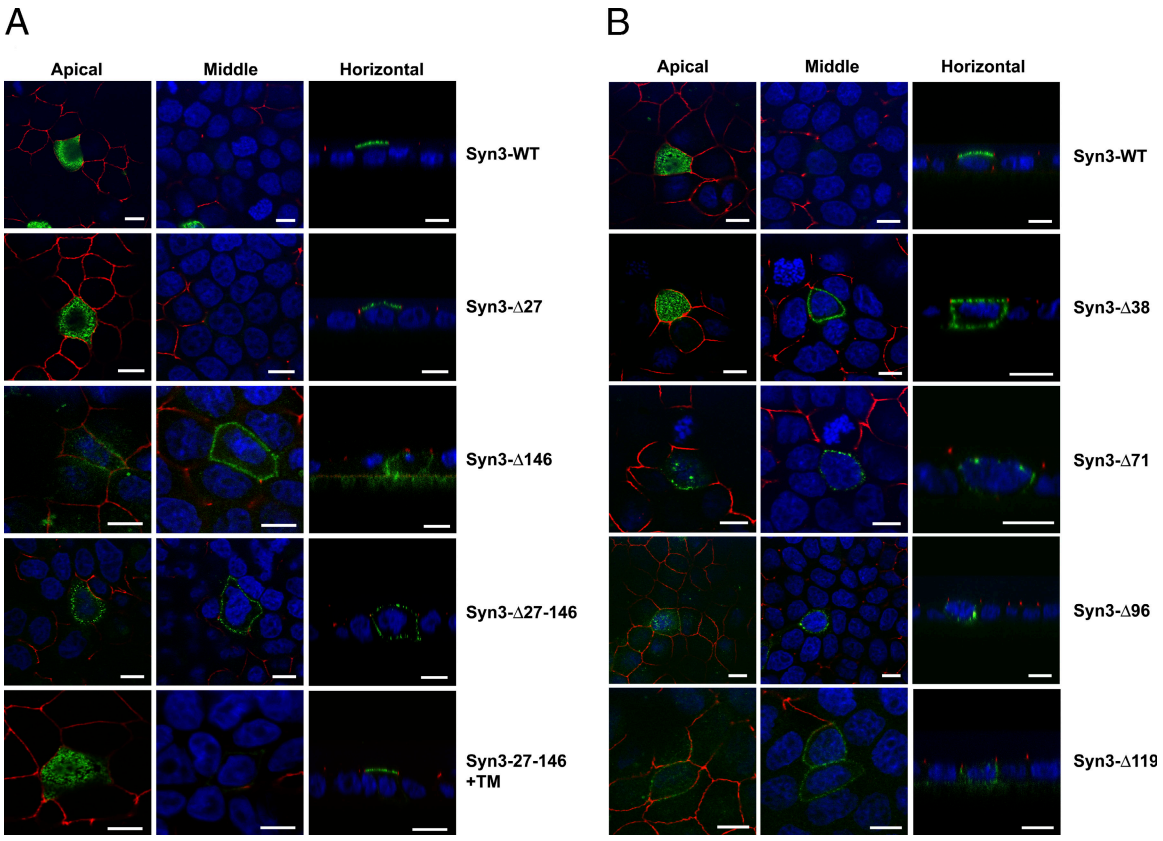

Figure 2. **The H_{abc} domain of syntaxin 3 contains a necessary and sufficient apical targeting signal centered around residues 27–38.** Syntaxin 3 mutants transiently transfected in MDCK cells were detected by surface-immunostaining and confocal microscopy. Syntaxin 3, green; the tight junction protein ZO-1, red; nuclei, blue. Representative XY optical sections of the apical region of the cells (left) or the middle of the cells (middle) are shown together with XZ optical sections (right). Results shown in Figs. 2 and 3 are representative images of at least 75–100 analyzed cells in at least five independent transfection experiments. Bars, 5 μm.

polarized targeting (Fig. 2 A). However, deletion of the H_{abc} domain (Syn3-Δ146), and any further deletion, results in loss of apical-specific targeting and random localization at the apical and basolateral domain (Fig. 2 A), indicating that the H_{abc} domain contains a necessary apical targeting signal. Fusing the H_{abc} domain directly to the transmembrane domain and omitting all other regions of syntaxin 3 (Syn3-27-146+TM) restores specific apical targeting (Fig. 2 A). These results indicate that the H_{abc} domain of syntaxin 3 contains a necessary and sufficient apical targeting signal.

To further locate this signal, we generated additional deletion mutants. The region of the syntaxin 3 gene encoding the H_{abc} domain contains four exon boundaries. Because exons often encode structural or functional domains, we designed deletion mutants according to their boundaries (Fig. 1 A). Deletion of the NH_2-terminal 38 residues (Syn3-Δ38) and any further deletion prevents specific apical targeting (Fig. 2 B), indicating that the region between residues 27–38 is critical.

Comparison of the primary structures of the four closely related plasma membrane syntaxins (1–4) revealed that this region contains a six-residue sequence (FMDEFF) that is conserved between syntaxins 1–3, but differs in syntaxin 4 (Fig. 3 A). The syntaxins 1–3 are known to target to the apical plasma membrane domain in polarized epithelial cells, whereas syntaxin 4 is strictly basolateral (Gaisano et al., 1996; Low et al., 1996, 2002; Quinones et al., 1999; Li et al., 2002). To test whether the FMDEFF motif is critical for apical targeting, we mutated each residue individually to an alanine. Three mutations (Syn3-F31A, D33A, and E34A) result in the loss of specific apical targeting, whereas the three others (Syn3-M32A, F35A, and F36A) behave like wild type (Fig. 3 B). This result indicates that the apical targeting signal of syntaxin 3 is centered around the first four residues (FMDE) of this conserved motif and that the residues F31, D33, and E34 play a critical role.

Mutation of the apical targeting signal of syntaxin 3 does not disrupt binding to SNAP-23

In neurons, syntaxin 1 binds to SNAP-25 to form a functional t-SNARE that can interact with the v-SNARE on synaptic vesicles. The interaction between syntaxin 1 and SNAP-25 depends solely on the SNARE domains of these proteins (Sutton et al., 1998). It has previously been reported that syntaxin 1 and SNAP-25 may be targeted to their final destination together in a complex, but this has been controversial (Salaun et al., 2004). SNAP-23 is a nonneuronal isoform of SNAP-25, binds to both syntaxin 3 and 4 (Ravichandran et al., 1996), and localizes to both the apical and basolateral plasma membrane in MDCK cells (Low et al., 1998b). To test whether mutagenesis of the apical targeting signal affects binding to SNAP-23, wild-type

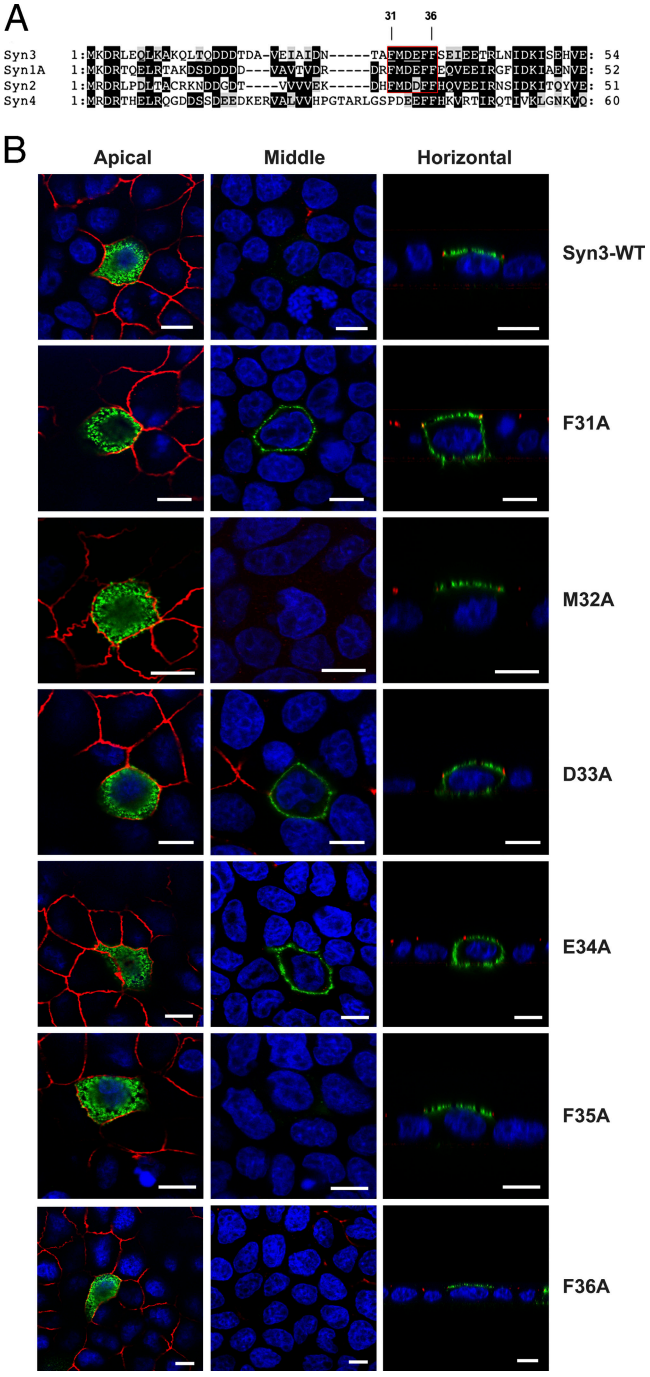

Figure 3. **A conserved FMDE motif is critical for apical targeting of syntaxin 3.** (A) Sequence alignment of the NH_2-terminal regions of human syntaxins 3, 1A, 2, and 4. Apically targeted syntaxins (1A, 2, and 3) contain a conserved motif (red box), which is different in the basolaterally targeted syntaxin 4. (B) Each residue of the FMDEFF motif of syntaxin 3 was individually changed to an alanine, and the effect on polarized targeting was tested as described in Fig. 2. Note that syn3-F31A, D33A, and E34A exhibit nonpolarized localization, indicating that these residues are critical for apical targeting. Bars, 5 μm.

syntaxin 3, Syn3-Δ38, and the six alanine point mutations were expressed in MDCK cells, which were immunoprecipitated using an anti-myc epitope antibody, and the binding to SNAP-23 was analyzed by immunoblotting. As shown in Fig. 4 A, wild-type syntaxin 3 and all mutants bind to SNAP-23 to a similar degree.

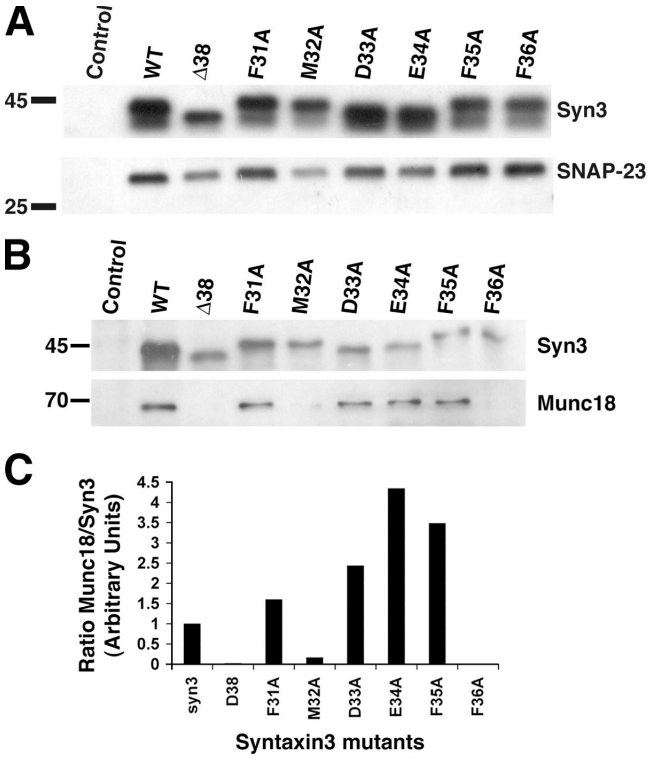

Figure 4. **Interaction with SNAP-23 and Munc18b.** MDCK cells were transiently transfected with myc-tagged, wild-type, or mutant syntaxin 3, immunoprecipitated using an anti-myc antibody, and then the binding of endogenous SNAP-23 (A) or Munc18b (B) was detected by immunoblotting. (C) Quantitation of data in B. Results represents the ratio for the synaptin 3–Munc18b signal intensities standardized to wt-syntaxin 3. Note that the apparent higher ratio for the synaptin 3–Munc18b binding of some of the mutants compared with wt-syntaxin 3 is likely caused by the higher expression level of the latter, which suggests a saturation effect.

This indicates that the loss of specific apical targeting in these mutants is not caused by an inability to bind to SNAP-23.

Apical targeting of syntaxin 3 is independent of binding to Munc18b

Members of the SM protein family regulate syntaxin function (Gallwitz and Jahn, 2003). In the case of syntaxin 1, the SM protein Munc18a has been shown to bind to a conformation in which the H_{abc} domain is tightly bound to the SNARE domain. Munc18a binding is thought to stabilize this closed conformation of syntaxin 1 and prevent interactions with other SNAREs. Munc18b is a nonneuronal homologue that specifically binds to syntaxin 3 in a region that includes its H_{abc} domain (Riento et al., 2000). Therefore, we tested whether binding to Munc18b may be required for the apical targeting of syntaxin 3. Wild-type syntaxin 3, Syn3-Δ38, and the six alanine point mutations were again expressed in MDCK cells, and Munc18b binding was analyzed by immunoprecipitation and immunoblotting. Wild-type syntaxin 3 coprecipitates with Munc18b, but Syn3-Δ38 does not (Fig. 4 B). Four of the point mutants (Syn3-F31A, D33A, E34A, and F35A) are able to bind to Munc18b, whereas two of the mutants lost binding activity (Syn3-M32A and F36A). However, the ability to bind to Munc18b does not correspond to the ability of the syntaxin 3 mutants to be correctly apically

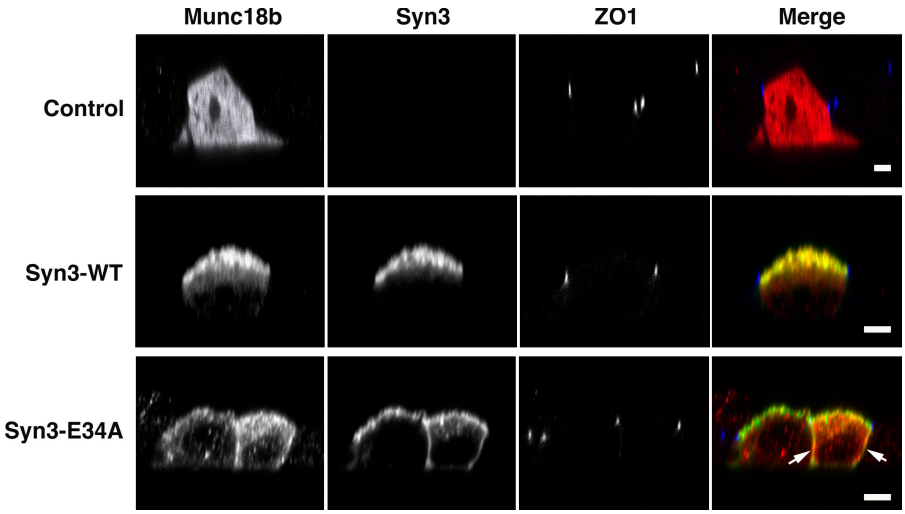

Figure 5. **Syntaxin 3 is required for polarized localization of Munc18b.** Munc18 alone or in combination with wt-syntaxin 3 or the E34A mutant were transiently expressed in MDCK cells. The localization of syntaxin 3 (green), Munc18b (red), and ZO-1 (blue) were analyzed by confocal immunofluorescence microscopy. Note that Munc18b alone exhibits cytoplasmic localization. Coexpression with wild-type syntaxin 3 results in apical localization of Munc18b, whereas coexpression of Syn3-E34A results in nonpolarized plasma membrane localization of Munc18b. Arrows indicate basolateral localization. Bars, 5 μm.

targeted. For example, Syn3-F31A, which is mislocalized, is still able to bind to Munc18b. In contrast, Syn3-F36A is properly apically localized, but has lost its ability to bind to Munc18b. This result indicates that apical targeting of syntaxin 3 is independent of its binding to Munc18b.

Next, we tested whether the localization of Munc18b in turn may be determined by the localization of syntaxin 3. Munc18b localizes to the apical plasma membrane of renal epithelial cells (Lehtonen et al., 1999). Because our available antibodies did not allow us to reliably detect the localization of endogenous Munc18b in MDCK cells, we transfected cells with epitope-tagged Munc18b. As shown in Fig. 5, Munc18b expressed alone exhibited a cytoplasmic distribution. However, cotransfection with wild-type syntaxin 3 resulted in colocalization of Munc18b with syntaxin 3 at the apical plasma membrane. In contrast, coexpression with the mistargeted syn3-E34A mutant resulted in membrane association of Munc18b in a nonpolarized manner. Altogether, these results indicate that both membrane-anchoring and the proper polarized localization of Munc18b depend on syntaxin 3.

Disruption of the apical targeting signal does not affect raft association of syntaxin 3

It has previously been reported that a fraction of syntaxin 3 can be recovered in detergent-insoluble membranes, and it was proposed that raft-association may play a role in apical targeting of syntaxin 3 (Lafont et al., 1999). We tested whether our syntaxin 3 mutants may fail to be properly targeted apically because of defective raft association. MDCK cells stably expressing wild-type syntaxin 3, syn3-Δ38, or wild-type syntaxin 4 as a control were subjected to detergent extraction and floatation gradient centrifugation, as previously described (Lafont et al., 1999). Caveolin-1 served as a raft-associated positive control and calnexin served as a nonraft control. As shown in Fig. 6, a large fraction of caveolin-1, but not calnexin, can be recovered in fraction 7 of the sucrose gradient. A smaller fraction of wild-type syntaxin 3 also partitions in this raft fraction, whereas syntaxin 4 does not. The syn3-Δ38 mutant partitions in the raft fractions to a similar extent as wild-type syntaxin 3. This result indicates that raft partitioning is not affected by deletion of the apical targeting signal of syntaxin 3. Therefore, although raft partitioning may be necessary for apical targeting of syntaxin 3, it is not sufficient.

A structural model of the apical targeting signal of syntaxin 3

3D structures of apical or basolateral targeting signals have not yet been clearly elucidated. The four-residue FMDE motif that we have identified as the apical targeting signal of syntaxin 3 is 100% conserved in syntaxin 1 (Fig. 3 A). The structure of the H_{abc} domain containing this motif has been reported for syntaxin 1 (Fernandez et al., 1998; Lerman et al., 2000). Assuming that the same motif is used for apical targeting of syntaxin 1 in epithelial cells, this would therefore be the first known 3D protein structure containing a signal involved in polarized targeting.

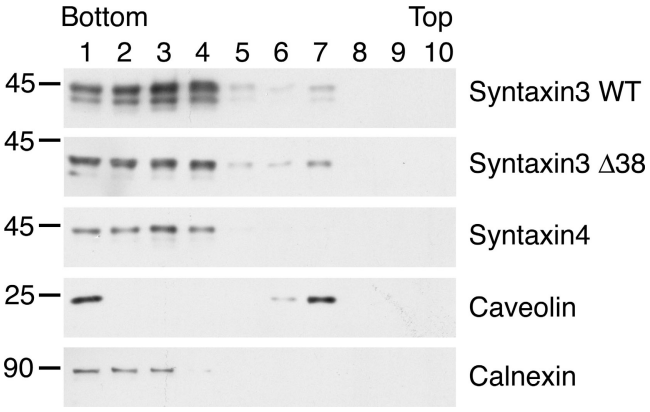

Figure 6. **Raft association of syntaxin 3 is unaffected by disruption of apical targeting signal.** MDCK cells stably expressing wt-syntaxin 3, syn3-Δ38, or syntaxin 4 were lysed in buffer containing 1% Triton X-100 and subjected to sucrose floatation gradient centrifugation. Collected fractions were analyzed by Western blot using the indicated antibodies. Note that a small fraction of both wt-syntaxin 3 and syn3-Δ38 cofractionate in rafts with caveolin-1 (fractions 6 and 7). In contrast, no significant raft association is detectable for syntaxin 4 under these conditions.

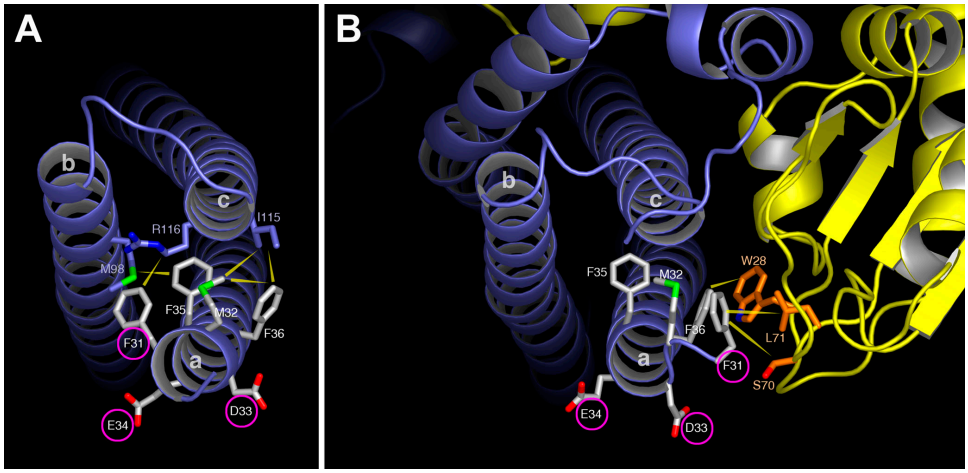

Figure 7. **Structural models of syntaxin 3, in isolation and in complex with Munc18b.** Residues of the FMDEFF motif are shown with white carbon atoms. Interactions are shown with yellow arrows. (A) Helices a–c of syntaxin 3 in isolation. Residues on helices b and c, which make contacts with residues of the FMDEFF motif, are shown with blue carbon atoms. F31, D33, and E34 (circled), which affect syntaxin 3 localization when mutated, are partially or fully exposed to solvent. (B) Model of syntaxin 3 in complex with Munc18b (yellow). Residues of Munc18b, which contact the FMDEFF motif are shown with orange carbons. Syn3-F31 makes hydrophobic contacts with Munc18b residues S70 and L71, whereas F36 contacts the Munc18b residue W28. Note that access to the FMDE apical targeting motif is partially shielded in the Munc18b complex as compared with the free syntaxin 3.

This allowed us to generate a model for the H_{abc} domain of syntaxin 3 using the syntaxin 1 structure as a template. As shown in Fig. 7 A, the side chains of all three critical residues, which affect localization (F31, D33, and E34), are exposed on the surface of the protein. This suggests that these residues may be contacted directly by a targeting factor recognizing this signal. The side chains of D33 and E34 are completely exposed, and one face of the F31 side chain is exposed. The other side of F31 faces the interior of the three-helical bundle formed by helices a–c, and potentially engages in a weak interaction with a methylene group of R116 on helix c.

All three residues of the FMDEFF motif, whose mutation has no effect on apical targeting (M32, F35, and F36), engage in hydrophobic interactions with side chains of the opposing helices b or c (Fig. 7 A). These residues may, thus, help to stabilize the three-helical bundle, but would be unlikely to interact with a putative apical sorting adaptor, which is consistent with our targeting results.

The crystal structure of the syntaxin 1–Munc18a complex has also been reported (Misura et al., 2000) and also contains the conserved FMDEFF motif. Therefore, we generated a model of the syntaxin 3–Munc18b complex, based on this crystal structure (Fig. 7 B). In the syntaxin 1A-Munc18a structure, the first turn of the "a" α-helix of syntaxin 1A is partially unwound, relative to the uncomplexed structure. We have modeled the syntaxin 3–Munc18b complex accordingly. In this model, F31 contacts S70 and L71 of Munc18b. It is therefore unlikely that F31, which is critical for apical targeting of syntaxin 3, would be accessible to a putative apical sorting adaptor if syntaxin 3 is in a complex with Munc18b. This is consistent with our data (Fig. 4 B), indicating that syntaxin 3 targeting is independent of Munc18b.

F36 interacts with W28 of Munc18b (Fig. 7 B). This extensive hydrophobic contact was also noted in a syntaxin 3–Munc18b model by Kauppi et al. (2002), and F36 is conserved in syntaxins 1–4. Our results verify that this contact is required for the association of syntaxin 3 and Munc18b (Fig. 4 B). Our results also showed that mutation of M32 substantially reduces the syntaxin 3–Munc18b interaction (Fig. 4 B). Our model does not suggest a direct basis for this effect because M32 is not located within contact distance of Munc18. However, the side chains of M32, F36, and F31 pack tightly together into a hydrophobic bundle. Thus, it is possible that M32 acts as a buttress for the side chains of F36 and F31, indirectly stabilizing their interactions with Munc18b.

Altogether, our structural analysis is consistent with a model in which the three residues critical for apical targeting of syntaxin 3 (F31, D33, and E43) directly interact with an apical sorting adaptor, and in which this interaction occurs with uncomplexed syntaxin 3, but not with the syntaxin 3–Munc18b complex.

Mislocalization of syntaxin 3 causes mistargeting of apical cargo

The three mistargeted point mutants (F31A, D33A, and E43A) of syntaxin 3 are likely to be fully functional because their SNARE domain is unaffected, and we observed normal binding to SNAP-23 and Munc18b. This allowed us to test the central aspect of the SNARE hypothesis, which is that SNARE pairing contributes to the specificity of vesicle-trafficking pathways. If correct, then the purposeful mistargeting of a t-SNARE to an aberrant location should make that location fusion-competent for transport vesicles carrying cargo intended for the original location of this t-SNARE. We investigated a cargo protein (p75-GFP) whose apical trafficking has previously been shown to depend on syntaxin 3 (Kreitzer et al., 2003). It was also shown that in polarized MDCK cells, apical post-Golgi vesicles carrying p75-GFP can reach the basolateral plasma membrane, presumably because of the infidelity of prior targeting mechanisms, but are unable to fuse there (Kreitzer et al., 2003). p75-GFP, which is transiently expressed in MDCK cells, targets to the

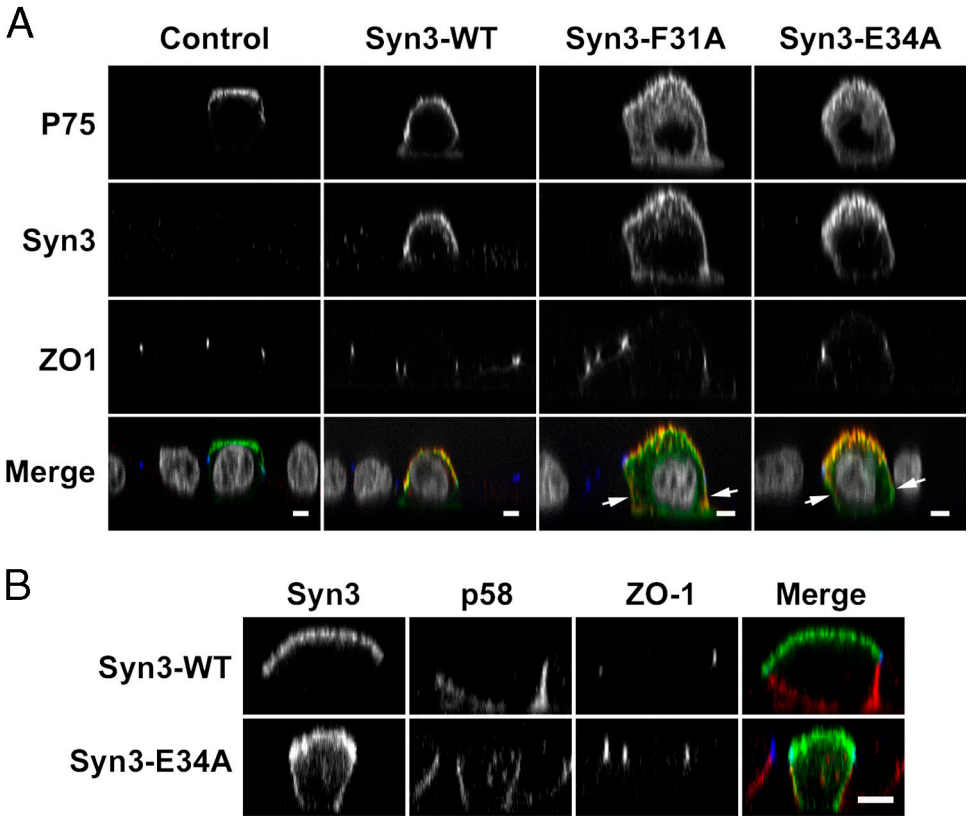

Figure 8. **Mistargeting of syntaxin 3 disrupts apical polarity of p75.** (A) The apically targeted p75-GFP was expressed alone or coexpressed with wild-type or mutant syntaxin 3. Syntaxin 3 (red), p75-GFP (green), and ZO-1 (blue) were detected by confocal immunofluorescence microscopy, and representative XZ optical sections are shown. Nuclei are shown in gray. p75-GFP alone targets to the apical plasma membrane. Expression of the mistargeted syntaxin 3 mutants F31A or E43A results in partial basolateral mislocalization of p75-GFP (arrows). (B) Expression of wt-syntaxin 3 or the E34A mutant (green) does not affect the basolateral localization of p58 (red). ZO-1, blue. Bars 5 μm.

apical plasma membrane (Fig. 8). As expected, cotransfection with wild-type syntaxin 3 does not change the apical polarity of p75-GFP. However, expression of mistargeted syntaxin mutants (F31A or E34A) resulted in partial mistargeting of p75-GFP to the basolateral plasma membrane (Fig. 8 A). In contrast, expression of mistargeted syntaxin 3 had no effect on the localization of the basolateral protein p58 (Fig. 8 B).

These results suggest that, under normal conditions, the absence of syntaxin 3 at the basolateral membrane renders this membrane fusion incompetent for apical cargo vesicles. However, if syntaxin 3 is supplied to the basolateral membrane, which is caused by disruption of its targeting signal, then this membrane becomes fusion competent and inappropriately accumulates apical membrane proteins. Therefore, these results strongly support the specificity aspect of the SNARE hypothesis.

Mislocalization of syntaxin 3 causes inhibition of epithelial polarity

We next asked whether the mistargeting of apical membrane proteins, which was induced by the expression of mistargeted syntaxin 3, would affect the cells' overall ability to acquire a polarized phenotype. The kinetics of the formation of tight junctions has frequently been used as a measure of the ability of epithelial cells to polarize. For example, disruption of "polarity proteins" such as PATJ, Par-1, and Par-6 in MDCK cells does not result in the complete inability to ultimately form a polarized monolayer, but, rather, causes a kinetic delay (Gao et al., 2002; Cohen et al., 2004; Shin et al., 2005). Therefore, we tested whether expression of mislocalized syntaxin 3 mutants would affect overall epithelial polarity in a similar fashion. We first cultured parental MDCK cells or cells stably transfected with syn3-E34A on permeable filters at high density for 2 d. Syntaxin expression was induced with doxycycline for 8 h, and cells were subjected to calcium-deficient medium for 15 h, which results in the opening of tight junctions. At time zero, cells were switched back to high calcium medium, and the reestablishment of tight junctions was monitored by measuring the transepithelial electrical resistance (TEER). As shown in Fig. 9 B, expression of syn3-E34A caused a significant delay of ~10 h in the characteristic peak of TEER indicative of tight junction reformation. This delay is similar to the effects observed with the disruption of polarity proteins such as PATJ and Par-6 (Gao et al., 2002; Shin et al., 2005). We also monitored tight junction reformation by immunofluorescence microscopy at different time points after calcium switch. As shown in Fig. 9 C, tight junctions are only incompletely formed in cells expressing syn3-E34A at 6 h after calcium switch, a time point at which control cells already exhibit extensive, circumferential immunostaining for the tight junction protein ZO-1. This effect of delaying the formation of tight junctions is similar to the effect observed by inhibition of

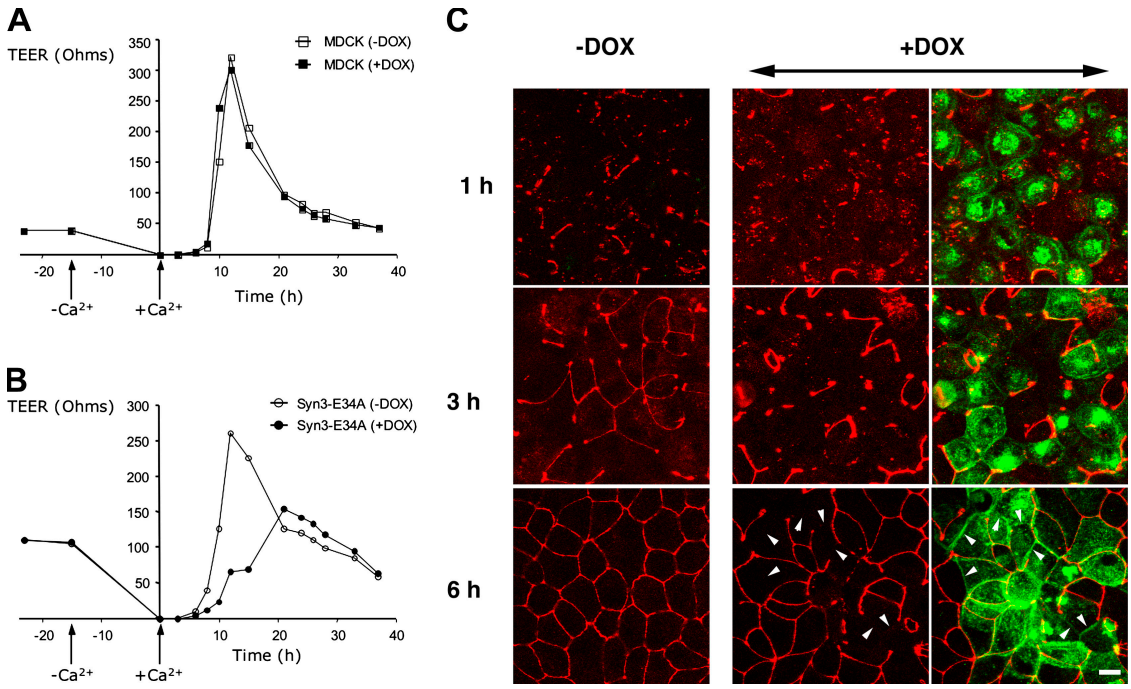

Figure 9. **Mistargeting of syntaxin 3 causes a delay in tight junction formation.** Parental MDCK cells or MDCK cells stably transfected for syn3-E43A were cultured on Transwell filters for 24 h, followed by induction with DOX for 8 h. Cultures were switched to low-calcium media for 15 h, resulting in the loss of tight junctions. Cultures were then switched back to normal calcium and the reestablishment of tight junctions was monitored by measuring the TEER (A and B) or by confocal immunofluorescence microscopy (C). (A and B) Reestablishment of tight junctions results in a characteristic peak of TEER at 12 h after calcium switch, which is significantly delayed in cells expressing the syn3-E34A. (C) Syn3-E34A transfected cells are stained for ZO-1 (red) and syntaxin 3 (green) at the indicated times after calcium switch. Representative projections of optical XY sections covering the entire apical areas of the cell layers are shown. After 6 h, most cells in the uninduced cultures (−DOX) exhibit circumferential tight junctions. In contrast, most cells expressing syn3-E43A (green) in the induced cultures (+DOX) exhibit incomplete tight junctions (arrowheads). Bar, 5 μm.

expression of the tight junction protein ZO-1 by RNAi (McNeil et al., 2006). These results suggest that syntaxin 3–dependent apical targeting pathways are involved in the polarization events necessary for tight junction formation.

Whereas disruption of proteins important for epithelial polarity often only results in a delay in polarization in a 2D culture system, as described above, MDCK cells are more sensitive when cultured in 3D collagen gels (O'Brien et al., 2001; Cohen et al., 2004; Shin et al., 2005). Therefore, we cultured MDCK cells in collagen gels for 7–9 d under conditions where they form spherical cysts in which the apical membrane faces a single lumen. Expression of wild-type syntaxin 3 did not interfere with the development of cysts (Fig. 10 A). In contrast, expression of syn3-E34A results in the inability to form organized cysts (Fig. 10). Instead, the cells formed tumor-like structures consisting of disorganized cells that were apparently unable to properly polarize and form a central lumen. Tight junctions were barely detectable or absent in these structures. This indicates that appropriately polarized syntaxin 3 plays a critical role in apicobasolateral epithelial polarization.

Discussion

We have identified a region centered around a conserved motif at the beginning of the H_{abc} domain of syntaxin 3 as a necessary and sufficient apical targeting signal. In contrast to basolateral targeting signals, the structure and function of apical targeting signals are not well understood. Basolateral targeting signals are typically found in cytoplasmic domains of integral membrane proteins, and some of these signals are thought to be recognized by clathrin adapters at the level of the Golgi apparatus and/or endosomes. In contrast, most known apical targeting signals do not reside in cytoplasmic domains of membrane proteins. Glycosylphosphatidylinositol anchors and lumenal glycosylation sites have been shown to confer apical targeting information on some proteins. Syntaxin 3 is neither glycosylphosphatidylinositol anchored nor does it possess a lumenal domain. Raft association mediated by transmembrane domains, and possibly by adjacent regions, has been implicated in apical targeting of other membrane proteins. Our results indicate that neither raft-association nor the transmembrane domain of syntaxin 3 are involved in apical targeting. Only recently, apical targeting signals in cytoplasmic domains of a handful of membrane proteins have been identified (Altschuler et al., 2003; Muth and Caplan, 2003; Rodriguez-Boulan et al., 2004). Interestingly, the cytoplasmic tails of both CFTR and rhodopsin can target to the apical membrane in the absence of transmembrane domains (Chuang and Sung, 1998; Milewski et al., 2001). In the case of CFTR, this depends on a COOH-terminal PDZ-binding domain, suggesting a mechanism of selective retention at the apical plasma membrane. Apical targeting of the GABA transporter GAT-3 (Muth et al., 1998) also depends on a COOH-terminal PDZ-binding motif, suggesting a common mechanism. However, this mechanism is clearly different from

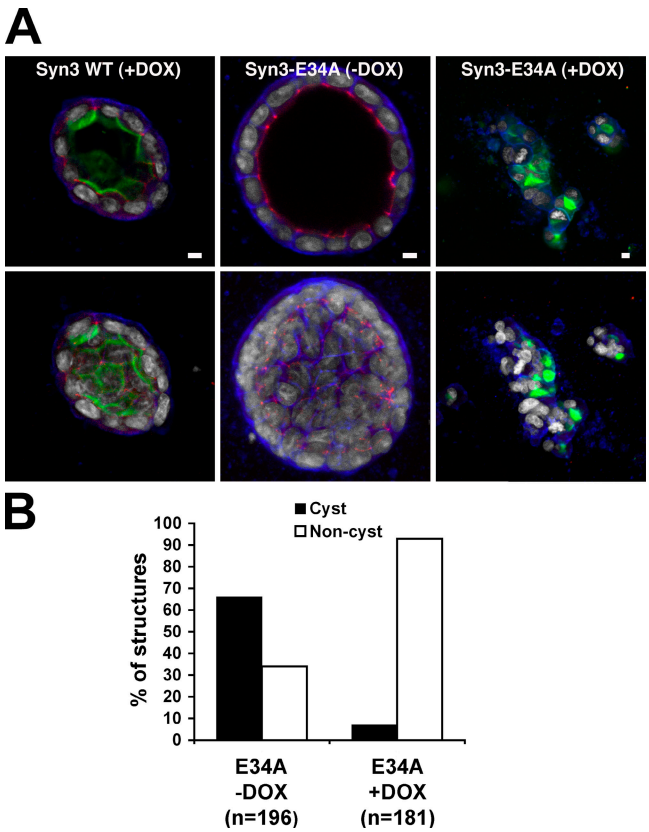

Figure 10. **Expression of mistargeted syntaxin 3 causes disruption of cell polarity.** (A) MDCK cells stably transfected for wt-syntaxin 3 or syn3-E34A were cultured in 3D collagen. Syntaxin expression was induced with DOX after 2 d of seeding, and culture was continued for an additional 6 d. Cells were fixed and immunostained for syntaxin 3 (green), ZO-1 (red), the basolateral marker p58 (blue), and DNA (white). The images show either single optical confocal sections of representative cell structures (top) or projections of half of the structures (bottom). Control cells (syn3-E34A and −DOX) or cells expressing wt-syntaxin 3 form ordered cysts consisting of polarized cells facing a single lumen. In contrast, expression of syn3-E34A (+DOX) leads to inability to form organized cysts. Instead, cells form tumor-like cell structures that lack tight junctions and exhibit no apparent cell polarity. Bars, 5 μm. (B) Quantitation of cyst formation. Cysts consisting of polarized cells or disorganized "noncysts" consisting of nonpolarized cells (as shown in A) were counted and are expressed as the percentage of total structures. Expression (+DOX) of Syn3-E34A results in the near inability of cells to form organized cysts.

the apical targeting of syntaxin 3, which does not possess a PDZ-binding domain. Several other diverse cytoplasmic apical targeting signals have been identified in polytopic membrane proteins, but this has not yet led to the identification of a possible common mechanism.

Only one potential secondary structure has been reported for the apical targeting signal of a bile acid transporter (Sun et al., 2003). Based on NMR analysis of a synthetic peptide, this has revealed a possible β-turn conformation of a four-residue sequence. Fortuitously, the apical targeting signal that we identified in syntaxin 3 falls in a region that is identical to that of syntaxin 1, whose crystal structure has been solved both for the free protein and for a complex with Munc18. This has allowed us to obtain the first structural model of any polarized targeting signal in the context of the bulk of the protein. The three critical residues that we have identified are all exposed on the surface of a triple-helix structure (Fig. 7) and should be accessible for interaction with a putative apical sorting adaptor. Altogether, the targeting motif of syntaxin 3 appears to differ from all other known polarized targeting signals and its characterization may aid in the identification of the machinery required for its recognition.

Our results indicate that Munc18b is not involved in the apical targeting of syntaxin 3, even though it binds to a region that overlaps with the identified apical targeting signal. The targeting phenotype of our Ala mutants does not correlate with their ability to bind to Munc18b (Fig. 4 B). Furthermore, structural modeling suggests that access to the apical targeting signal would be partially blocked in the syntaxin 3–Munc18b complex (Fig. 7). Therefore, we suggest that syntaxin 3 and Munc18b are not targeted together as a complex. This conclusion is consistent with the recent finding that the synaptic targeting of syntaxin 1 is not affected in Munc18a-null animals (Toonen et al., 2005). Our experiments (Fig. 5) indicate that both membrane-association and apical polarity of Munc18b depend on syntaxin 3 and that it does not contain any polarized targeting information in itself.

Interestingly, the FMDE motif of syntaxin 3 overlaps with the predicted binding site on syntaxin 1 (FMDEFFEQVE) of botulinum neurotoxin C (Rossetto et al., 1994). This toxin inactivates syntaxin 1 by proteolytic cleavage. Syntaxin 3 is also subject to botulinum neurotoxin C cleavage (Schiavo et al., 1995), suggesting that the same region is recognized. Therefore, we suggest that bacterial neurotoxins, to specifically recognize SNARE proteins, evolved to exploit the exposed domains in SNAREs, which were originally meant for the binding of adaptor proteins that were essential for their subcellular targeting. Another example may be VAMP2, which is recognized by botulinum neurotoxin D in the same region (Pellizzari et al., 1997); it was shown to be required for targeting to synaptic vesicles and endocytosis (Grote et al., 1995), although this coincidence was not recognized.

Based on the few cases in which targeting signals of other syntaxins have been identified, one can conclude that there is not a single conserved region that generally contains the signals. The Golgi-targeting signal of syntaxin 5 is contained within its SNARE domain. This domain targets to the Golgi, even in the absence of the transmembrane domain (Misumi et al., 2001). In contrast, a longer splice isoform of syntaxin 5 contains an NH_2-terminal ER retrieval signal (Hui et al., 1997). The localization of syntaxin 6 to the TGN also depends on its SNARE domain, but there is an additional tyrosine-based signal in the middle of the molecule that may act as an internalization signal to facilitate the retrieval of syntaxin 6 back to the TGN (Watson and Pessin, 2000). Finally, the retention in the ER membrane of the yeast syntaxin Ufe1p depends only on the length, but not the sequence, of its transmembrane domain (Rayner and Pelham, 1997).

The region containing the apical targeting signal in syntaxin 3 has not previously been implicated in the targeting of a syntaxin. However, given that the critical FMDE motif is also conserved in syntaxins 1 and 2 suggests that it may also be used in apical targeting of these syntaxins. Syntaxin 2 has been

shown to target to the apical membrane of pancreatic acinar cells (Gaisano et al., 1996). In the kidney, syntaxin 2 localizes to the apical domain of medullary collecting duct cells, but to the basolateral domain of cortical-collecting duct principal cells (Li et al., 2002). Furthermore, syntaxin 2 localizes to the basolateral domain of retinal pigment epithelial cells (Low et al., 2002). This suggests that syntaxin 2 may contain a competing basolateral targeting signal that is recognized in a cell type–dependent fashion. MDCK cells target syntaxin 2 to both the apical and basolateral domain (Low et al., 1996; Quinones et al., 1999), which may suggest that they can recognize both signals. Whether the FMDE-motif of syntaxin 1 is involved in neuronal targeting remains to be determined.

It is now widely accepted that SNAREs are intimately involved in the mechanism of fusion. The question of specificity, however, had been controversial since it was found that SNAREs in solution can bind promiscuously (Yang et al., 1999). Subsequent results from in vitro reconstituted fusion assays with artificial liposomes established that membrane-anchored SNAREs allow only fusion of cognate SNARE complexes (McNew et al., 2000). Our results provide evidence that SNARE pairing also contributes to the overall specificity of trafficking pathways in intact cells. Our results are consistent with a model in which the mislocalization of functional syntaxin 3 to the "incorrect" basolateral membrane makes this membrane permissive for fusion of apical post-Golgi vesicles and leads to the incorrect basolateral delivery of apical proteins. As previously shown by time-lapse imaging of post-Golgi transport vesicles in polarized MDCK cells, the fidelity of targeting of p75-GFP is not absolute, and vesicles carrying p75-GFP can reach the basolateral membrane, but are unable to fuse there (Kreitzer et al., 2003). Our results suggest that the expression of mistargeted mutants of syntaxin 3 renders the basolateral membrane fusion competent for such vesicles, which results in the accumulation of p75-GFP at the basolateral domain (Fig. 8). This strongly supports the notion that SNARE pairing contributes to the overall specificity of membrane trafficking pathways in vivo and suggests that SNARE-mediated membrane fusion acts as a final proofreading mechanism to allow the fusion of "correct" vesicles and deny the fusion of incorrect vesicles with a given target membrane.

The effect of mistargeting of syntaxin 3 to the basolateral domain strikingly resembles the defects of apicobasolateral polarity caused by the disruption of so-called polarity proteins. Proteins such as PATJ, Par-1, and Par-6 have been shown to be important for epithelial polarity (Gao et al., 2002; Cohen et al., 2004; Shin et al., 2005). Their inactivation, usually by siRNA, typically results in kinetic delays in tight junction formation in MDCK cells cultured on permeable filters. For unknown reasons, cell polarity is more severely affected when MDCK cells are cultured in 3D collagen. In the case of syntaxin 3, we find that merely disrupting its specific apical targeting results in a dominant effect that causes polarity defects very similar to those caused by inactivating PATJ, Par-1, Par-6, and other polarity proteins. This indicates that not just the function of syntaxin 3 but also its apical-specific localization is essential for epithelial polarity.

Materials and methods

Cell culture and transfection

MDCK clone #11 cells were used for all experiments. These cells were made from MDCK strain II cells by stable transfection with the tetracycline repressor (Invitrogen), cloning, and extensive characterization of tetracycline inducibility and epithelial polarity parameters. These cells were used for subsequent stable transfections using pcDNA4-TO plasmids (Invitrogen) for tetracycline-inducible expression of proteins of interest. Cells were maintained in MEM containing 5% FBS and penicillin/streptomycin at 37°C and 5% CO_2. For transgene induction, the cells were induced with 50 ng/ml of the tetracycline analogue doxycycline for at least 16 h. For microscopy studies with polarized syntaxin 3 mutants, the cells were grown on polycarbonate filters (12-mm diam; 0.4 μM pore size; Costar Corning) for at least 48 h.

For transient transfections, cells were seeded on Transwell filters and immediately mixed with the transfection agent Exgen500 (Fermentas) and plasmid DNA in 500 μl of media containing 15% FBS. Fresh media with or without doxycycline was added after 6 h of transfection. The cells were cultured for a total of 48 h, until they were polarized. All transient transfection experiments were repeated at least three times. Stable transfection was done by calcium phosphate precipitation with linearized plasmids, and stable clones were selected using Zeocin.

For culture in 3D collagen gels, MDCK cells were seeded from 0.5 to 10^4 cells/ml in 80% collagen (Vitrogen) and 20% MEM containing 0.02 M Hepes, pH 7.4, and 0.02 M $NaHCO_3$ on either 16-well chambered slides (Lab-Tek; Nunc) or on 0.2 μm membrane inserts (Anapore; Nunc). The filters were kept at 37°C for 30 min to solidify the collagen, after which media containing 5% FBS and penicillin/streptomycin was added. Gene expression was induced by adding doxycycline after 2 d of seeding, and the cultures were continued for a total of 7–10 d.

Mutagenesis

All expression constructs are based on human syntaxin 3, using a modified pcDNA4-TO expression vector for the addition of two COOH-terminal myc epitope tags and one hexa-histidine tag. Deletion mutants were made by PCR. Point mutants were generated using complementary sense and antisense primers containing the desired mutation in the middle of the primers. PCR products were digested with the enzyme DpnI before cloning into the expression vector. All inserts were confirmed by sequencing.

Surface delivery assay

An assay for the quantitation of the kinetics of surface delivery of newly synthesized syntaxin 3 was established by modification of a protocol for measuring surface delivery of the polymeric immunoglobulin receptor in MDCK cells (Low et al., 1998a). In brief, MDCK cells that stably express myc-tagged syntaxin 3 were cultured on transwell filters for 3 d. After 12 h of induction with doxycycline for the expression of syntaxin 3, cells were starved for 30 min in methionine-deficient media (DMEM; Invitrogen). After starvation, cells were metabolically labeled for 15 min with [^{35}S]methionine (GE Healthcare), followed by a chase with unlabeled methionine for different time intervals. Anti-myc antibody was present throughout the chase, in either the apical or basolateral media compartment. Antibody binding was allowed to proceed for 60 min on ice, after which excess antibody was washed away. Cells were lysed in a buffer containing Triton X-100 with the addition of MDCK cell lysates containing an excess of unlabeled myc-tagged syntaxin. Antibody-tagged syntaxin molecules that had been exposed to the surface were precipitated with protein G–Sepharose. The remaining syntaxin molecules that had not reached the surface were subsequently immunoprecipitated with fresh antibody and protein G–Sepharose. Immunoprecipitates were separated by SDS-PAGE, gels were dried, and radioactive bands were imaged using a Molecular Imager FX (Bio-Rad Laboratories). Images were quantitatively analyzed using Quantity One analyzing software (Bio-Rad Laboratories).

Immunocytochemistry

For surface staining, MDCK cells on Transwell filters were incubated on ice for 1 h with the anti-myc epitope antibody 9E10 diluted in MEM containing 20 mM Hepes and 0.6% BSA with gentle shaking. The cells were washed with MEM four times for 10 min. Afterward, the cells were fixed with 4% paraformaldehyde at 4°C for 25 min. After quenching in PBS containing 75 mM ammonium chloride and 25 mM glycine, cells were permeabilized with PBS containing 3% BSA and 0.2% Triton X-100. Filters were cut out and incubated with primary antibodies for 1 h at 37°C, followed by fluorescence-labeled secondary antibodies.

For immunostaining of MDCK cells in 3D collagen cultures, the collagen was digested with 100 U/ml of collagenase type VII (Sigma-Aldrich) for 10 min. After digestion, gels were fixed with 4% paraformaldehyde (Sigma-Aldrich) for 30 min. Immunostaining was done with extended primary and secondary antibody incubation times and washing (24 h incubation for antibodies and four 30-min washes). Gels were mounted using antifade reagent (ProLong Gold; Invitrogen).

Images were acquired with a confocal microscope (TCS-SP2; Leica) at room temperature using a 63×, 1.4 NA, or a 20×, 0.7 NA, lens. Projection images were constructed using Leica confocal software. Using Photoshop software (Adobe), histograms were linearly adjusted for optimal representation of the 8-bit signals, individual channels were overlaid in RGB images, and composites of panels were made for final figures.

Coimmunoprecipitation

MDCK cells were transiently transfected with myc-tagged syntaxin 3 plasmids. After 24 h, cells were lysed in buffer containing Triton X-100, and syntaxin 3 was immunoprecipitated with cross-linked 9E10 antibody. Syntaxin 3 was detected by Western blot using an affinity-purified polyclonal antibody made against a GST fusion protein with human syntaxin 3. Munc18b was detected by a polyclonal antibody (Affinity BioReagents). A polyclonal antibody against a COOH-terminal peptide of SNAP-23 has been previously described (Low et al., 1998b).

Structural modeling

Homology models of syntaxin 3 and a syntaxin 3–Munc18b complex were constructed using structures of syntaxin 1A (PDB:1EZ3; Lerman et al., 2000) and a syntaxin 1–Munc18a complex (PDB:1DN1; ref 2) as templates. Models were constructed and optimized using the Swiss-Model website (Schwede et al., 2003) in project mode. Structures were minimized in the SwissPBDViewer program (Guex and Peitsch, 1997), and side chains of residues making obvious clashes were adjusted using rotamers from an extended rotamer library (Lovell et al., 2000) in the program O (Jones and Kjeldgard, 1997). Figures were generated using PyMOL (Delano, W.L.; http://www.pymol.org).

We thank Zhizhou Zhang and Elisabeth Loh for help with initial experiments.

This work was supported by a grant from the National Institutes of Health to T. Weimbs (R01GM66785) and a Predoctoral Fellowship from the American Heart Association to N. Sharma.

Submitted: 24 March 2006
Accepted: 17 May 2006

References

Altschuler, Y., C. Hodson, and S.L. Milgram. 2003. The apical compartment: trafficking pathways, regulators and scaffolding proteins. *Curr. Opin. Cell Biol.* 15:423–429.

Chen, Y.A., and R.H. Scheller. 2001. SNARE-mediated membrane fusion. *Nat. Rev. Mol. Cell Biol.* 2:98–106.

Chuang, J.Z., and C.H. Sung. 1998. The cytoplasmic tail of rhodopsin acts as a novel apical sorting signal in polarized MDCK cells. *J. Cell Biol.* 142:1245–1256.

Cohen, D., P.J. Brennwald, E. Rodriguez-Boulan, and A. Musch. 2004. Mammalian PAR-1 determines epithelial lumen polarity by organizing the microtubule cytoskeleton. *J. Cell Biol.* 164:717–727.

Fernandez, I., J. Ubach, I. Dulubova, X. Zhang, T.C. Sudhof, and J. Rizo. 1998. Three-dimensional structure of an evolutionarily conserved N-terminal domain of syntaxin 1A. *Cell*. 94:841–849.

Gaisano, H.Y., M. Ghai, P.N. Malkus, L. Sheu, A. Bouquillon, M.K. Bennett, and W.S. Trimble. 1996. Distinct cellular locations and protein-protein interactions of the syntaxin family of proteins in rat pancreatic acinar cells. *Mol. Biol. Cell*. 7:2019–2027.

Gallwitz, D., and R. Jahn. 2003. The riddle of the Sec1/Munc-18 proteins - new twists added to their interactions with SNAREs. *Trends Biochem. Sci.* 28:113–116.

Gao, L., G. Joberty, and I.G. Macara. 2002. Assembly of epithelial tight junctions is negatively regulated by Par6. *Curr. Biol.* 12:221–225.

Grote, E., J.C. Hao, M.K. Bennett, and R.B. Kelly. 1995. A targeting signal in VAMP regulating transport to synaptic vesicles. *Cell*. 81:581–589.

Guex, N., and M.C. Peitsch. 1997. SWISS-MODEL and the Swiss-PdbViewer: an environment for comparative protein modeling. *Electrophoresis*. 18:2714–2723.

Hui, N., N. Nakamura, B. Sonnichsen, D.T. Shima, T. Nilsson, and G. Warren. 1997. An isoform of the Golgi t-SNARE, syntaxin 5, with an endoplasmic reticulum retrieval signal. *Mol. Biol. Cell*. 8:1777–1787.

Jahn, R., T. Lang, and T.C. Sudhof. 2003. Membrane fusion. *Cell*. 112:519–533.

Jones, T.A., and M. Kjeldgard. 1997. Electron-density map interpretation. *Methods Enzymol.* 277:173–208.

Kauppi, M., G. Wohlfahrt, and V.M. Olkkonen. 2002. Analysis of the Munc18b-syntaxin binding interface. Use of a mutant Munc18b to dissect the functions of syntaxins 2 and 3. *J. Biol. Chem.* 277:43973–43979.

Kreitzer, G., J. Schmoranzer, S.H. Low, X. Li, Y. Gan, T. Weimbs, S.M. Simon, and E. Rodriguez-Boulan. 2003. Three-dimensional analysis of post-Golgi carrier exocytosis in epithelial cells. *Nat. Cell Biol.* 5:126–136.

Lafont, F., P. Verkade, T. Galli, C. Wimmer, D. Louvard, and K. Simons. 1999. Raft association of SNAP receptors acting in apical trafficking in Madin-Darby canine kidney cells. *Proc. Natl. Acad. Sci. USA*. 96:3734–3738.

Lehtonen, S., K. Riento, V.M. Olkkonen, and E. Lehtonen. 1999. Syntaxin 3 and Munc-18-2 in epithelial cells during kidney development. *Kidney Int.* 56:815–826.

Lerman, J.C., J. Robblee, R. Fairman, and F.M. Hughson. 2000. Structural analysis of the neuronal SNARE protein syntaxin-1A. *Biochemistry*. 39:8470–8479.

Li, X., S.H. Low, M. Miura, and T. Weimbs. 2002. SNARE expression and localization in renal epithelial cells suggest mechanism for variability of trafficking phenotypes. *Am. J. Physiol. Renal Physiol.* 283:F1111–F1122.

Lovell, S.C., J.M. Word, J.S. Richardson, and D.C. Richardson. 2000. The penultimate rotamer library. *Proteins*. 40:389–408.

Low, S.H., S.J. Chapin, T. Weimbs, L.G. Kömüves, M.K. Bennett, and K.E. Mostov. 1996. Differential localization of syntaxin isoforms in polarized MDCK cells. *Mol. Biol. Cell*. 7:2007–2018.

Low, S.H., S.J. Chapin, C. Wimmer, S.W. Whiteheart, L.K. Kömüves, K.E. Mostov, and T. Weimbs. 1998a. The SNARE machinery is involved in apical plasma membrane trafficking in MDCK cells. *J. Cell Biol.* 141:1503–1513.

Low, S.H., P.A. Roche, H.A. Anderson, S.C. van Ijzendoorn, M. Zhang, K.E. Mostov, and T. Weimbs. 1998b. Targeting of SNAP-23 and SNAP-25 in polarized epithelial cells. *J. Biol. Chem.* 273:3422–3430.

Low, S.H., L.Y. Marmorstein, M. Miura, X. Li, N. Kudo, A.D. Marmorstein, and T. Weimbs. 2002. Retinal pigment epithelial cells exhibit unique expression and localization of plasma membrane syntaxins which may contribute to their trafficking phenotype. *J. Cell Sci.* 115:4545–4553.

McNeil, E., C. Capaldo, and I.G. Macara. 2006. Zonula occludens-1 function in the assembly of tight junctions in Madin-Darby canine kidney epithelial cells. *Mol. Biol. Cell*. 17:1922–1932.

McNew, J.A., F. Parlati, R. Fukuda, R.J. Johnston, K. Paz, F. Paumet, T.H. Sollner, and J.E. Rothman. 2000. Compartmental specificity of cellular membrane fusion encoded in SNARE proteins. *Nature*. 407:153–159.

Milewski, M.I., J.E. Mickle, J.K. Forrest, D.M. Stafford, B.D. Moyer, J. Cheng, W.B. Guggino, B.A. Stanton, and G.R. Cutting. 2001. A PDZ-binding motif is essential but not sufficient to localize the C terminus of CFTR to the apical membrane. *J. Cell Sci.* 114:719–726.

Misumi, Y., M. Sohda, A. Tashiro, H. Sato, and Y. Ikehara. 2001. An essential cytoplasmic domain for the Golgi localization of coiled-coil proteins with a COOH-terminal membrane anchor. *J. Biol. Chem.* 276:6867–6873.

Misura, K.M., R.H. Scheller, and W.I. Weis. 2000. Three-dimensional structure of the neuronal-Sec1-syntaxin 1a complex. *Nature*. 404:355–362 (see comments).

Mostov, K., T. Su, and M. ter Beest. 2003. Polarized epithelial membrane traffic: conservation and plasticity. *Nat. Cell Biol.* 5:287–293.

Muth, T.R., and M.J. Caplan. 2003. Transport protein trafficking in polarized cells. *Annu. Rev. Cell Dev. Biol.* 19:333–366.

Muth, T.R., J. Ahn, and M.J. Caplan. 1998. Identification of sorting determinants in the C-terminal cytoplasmic tails of the gamma-aminobutyric acid transporters GAT-2 and GAT-3. *J. Biol. Chem.* 273:25616–25627.

O'Brien, L.E., T.S. Jou, A.L. Pollack, Q. Zhang, S.H. Hansen, P. Yurchenco, and K.E. Mostov. 2001. Rac1 orientates epithelial apical polarity through effects on basolateral laminin assembly. *Nat. Cell Biol.* 3:831–838.

Pellizzari, R., S. Mason, C.C. Shone, and C. Montecucco. 1997. The interaction of synaptic vesicle-associated membrane protein/synaptobrevin with botulinum neurotoxins D and F. *FEBS Lett.* 409:339–342.

Quinones, B., K. Riento, V.M. Olkkonen, S. Hardy, and M.K. Bennett. 1999. Syntaxin 2 splice variants exhibit differential expression patterns, biochemical properties and subcellular localizations. *J. Cell Sci.* 112:4291–4304.

Ravichandran, V., A. Chawla, and P.A. Roche. 1996. Identification of a novel syntaxin- and synaptobrevin/VAMP-binding protein, SNAP-23, expressed in non-neuronal tissues. *J. Biol. Chem.* 271:13300–13303.

Rayner, J.C., and H.R. Pelham. 1997. Transmembrane domain-dependent sorting of proteins to the ER and plasma membrane in yeast. *EMBO J.* 16:1832–1841.

Riento, K., M. Kauppi, S. Keranen, and V.M. Olkkonen. 2000. Munc18-2, a functional partner of syntaxin 3, controls apical membrane trafficking in epithelial cells. *J. Biol. Chem.* 275:13476–13483.

Rodriguez-Boulan, E., A. Musch, and A. Le Bivic. 2004. Epithelial trafficking: new routes to familiar places. *Curr. Opin. Cell Biol.* 16:436–442.

Rodriguez-Boulan, E., G. Kreitze, and A. Musch. 2005. Organization of vesicular trafficking in epithelia. *Nat. Rev. Mol. Cell Biol.* 6:233–247.

Rossetto, O., G. Schiavo, C. Montecucco, B. Poulain, F. Deloye, L. Lozzi, and C.C. Shone. 1994. SNARE motif and neurotoxins. *Nature*. 372:415–416 (letter).

Rothman, J.E., and G. Warren. 1994. Implications of the SNARE hypothesis for intracellular membrane topology and dynamics. *Curr. Biol.* 4:220–233.

Salaun, C., D.J. James, J. Greaves, and L.H. Chamberlain. 2004. Plasma membrane targeting of exocytic SNARE proteins. *Biochim. Biophys. Acta*. 1693:81–89.

Scales, S.J., Y.A. Chen, B.Y. Yoo, S.M. Patel, Y.C. Doung, and R.H. Scheller. 2000. SNAREs contribute to the specificity of membrane fusion. *Neuron*. 26:457–464.

Schiavo, G., C.C. Shone, M.K. Bennett, R.H. Scheller, and C. Montecucco. 1995. Botulinum neurotoxin type C cleaves a single Lys-Ala bond within the carboxyl-terminal region of syntaxins. *J. Biol. Chem.* 270:10566–10570.

Schwede, T., J. Kopp, N. Guex, and M.C. Peitsch. 2003. SWISS-MODEL: An automated protein homology-modeling server. *Nucleic Acids Res.* 31:3381–3385.

Shin, K., S. Straight, and B. Margolis. 2005. PATJ regulates tight junction formation and polarity in mammalian epithelial cells. *J. Cell Biol.* 168:705–711.

Sun, A.Q., R. Salkar, Sachchidanand, S. Xu, L. Zeng, M.M. Zhou, and F.J. Suchy. 2003. A 14-amino acid sequence with a beta-turn structure is required for apical membrane sorting of the rat ileal bile acid transporter. *J. Biol. Chem*. 278:4000–4009.

Sutton, R.B., D. Fasshauer, R. Jahn, and A.T. Brunger. 1998. Crystal structure of a SNARE complex involved in synaptic exocytosis at 2.4 A resolution. *Nature*. 395:347–353.

Toonen, R.F., K.J. de Vries, R. Zalm, T.C. Sudhof, and M. Verhage. 2005. Munc18-1 stabilizes syntaxin 1, but is not essential for syntaxin 1 targeting and SNARE complex formation. *J. Neurochem.* 93:1393–1400.

Ungar, D., and F.M. Hughson. 2003. SNARE protein structure and function. *Annu. Rev. Cell Dev. Biol.* 19:493–517.

Watson, R.T., and J.E. Pessin. 2000. Functional cooperation of two independent targeting domains in syntaxin 6 is required for its efficient localization in the trans-golgi network of 3T3L1 adipocytes. *J. Biol. Chem.* 275:1261–1268.

Weimbs, T., S.H. Low, S.J. Chapin, and K.E. Mostov. 1997a. Apical targeting in polarized epithelial cells: there's more afloat than rafts. *Trends Cell Biol.* 7:393–399.

Weimbs, T., S.H. Low, S.J. Chapin, K.E. Mostov, P. Bucher, and K. Hofmann. 1997b. A conserved domain is present in different families of vesicular fusion proteins: A new superfamily. *Proc. Natl. Acad. Sci. USA*. 94:3046–3051.

Weimbs, T., K.E. Mostov, S.H. Low, and K. Hofmann. 1998. A model for structural similarity between different SNARE complexes based on sequence relationships. *Trends Cell Biol.* 8:260–262.

Yang, B., L. Gonzalez Jr., R. Prekeris, M. Steegmaier, R.J. Advani, and R.H. Scheller. 1999. SNARE interactions are not selective. Implications for membrane fusion specificity. *J. Biol. Chem.* 274:5649–5653.